ORIGINAL PAPER

A fluorometric and colorimetric method for determination of trypsin by exploiting the gold nanocluster-induced aggregation of hemoglobin-coated gold nanoparticles

Zhengming Zhou[1] · Wei Liu[1] · Yanying Wang[1] · Fang Ding[2] · Xiaopeng Liu[3] · Qingbiao Zhao[4] · Ping Zou[1] · Xianxiang Wang[1] · Hanbing Rao[1]

Abstract

A dual-signal assay is described for the determination of trypsin based on the use of gold nanoparticles (AuNPs) that aggregate in the presence of gold nanoclusters (AuNCs) due to electrostatic interaction. This is accompanied by a color change from red to blue. However, if hemoglobin (Hb) is present in the solution, it will attach to the surface of AuNPs, thus preventing aggregation. The Hb-coated AuNPs quench the fluorescence of AuNCs. Trypsin can hydrolyze Hb and destroy the protective coating of Hb on the AuNPs. As a result, AuNP aggregation will occur after the addition of AuNCs, and the blue fluorescence of the AuNCs with 365 nm excitation and 455 nm maximum emission peak is recovered. Thus, trypsin can be determined by measurement of fluorescence emission intensity. Additionally, trypsin can be determined by the maximum absorption peak wavelength between 530 nm and 610 nm. Fluorescence increases linearly in the 10–2500 ng·mL^{-1} concentration range, and absorbance in the 20–2000 ng·mL^{-1} concentration range. The limits of detection are 4.6 ng·mL^{-1} (fluorometry) and 8.4 ng·mL^{-1} (colorimetry), respectively. The assay is sensitive and selective, and can be applied to the determination of trypsin in serum.

Keywords Dual-signal assay · Fluorescence resonance energy transfer · Hemoglobin coated gold nanoparticles · Fluorescence · Colorimetry · Electrostatic interaction · Serum analysis

Introduction

Proteases function as the catalyst for breaking the peptide bond in proteins [1, 2]. Trypsin belongs to the class of serine proteases that is produced in pancreas. It mainly functions in catalyzing the hydrolysis of arginine or lysine residues in C terminal [3]. The abnormal expression of trypsin will affect pancreatic function and lead to pathological consequences. Therefore, it is used as a reliable biomarker in acute

---

The authors wish it to be known that, in their opinions, Zhengming Zhou and Wei Liu should be regarded as joint First Authors.

Electronic supplementary material The online version of this article (https://doi.org/10.1007/s00604-019-3380-2) contains supplementary material, which is available to authorized users.

✉ Qingbiao Zhao
    qbzhao@ee.ecnu.edu.cn

✉ Hanbing Rao
    rhb@sicau.edu.cn

Extended author information available on the last page of the article

pancreatitis, cystic fibrosis and other diseases [4]. The determination of trypsin is essential in physiological and pathological diagnosis and treatment, and it is of significant importance to develop a sensitive and selective method for efficient and visible determination of trypsin.

Several approaches for determination of trypsin have been described. These include radioimmunoassays [5], electrophoresis [6] and high performance liquid chromatography [7]. These methods are relatively mature in technology and operation experience, which have been widely applied in scientific research and laboratory analysis. The colorimetric [8, 9] and fluorescent [10–13] determination of trypsin based on nanoprobe has attracted great attention compared with traditional detection methods owing to the simple instrumentation, convenient operation and direct observation. To date, several fluorescent or colorimetric methods for trypsin detection were established. Xue et al. [9] proposed a colorimetric label-free assay for trypsin detection by using gold nanoparticles. Miao et al. [8] developed a label-free colorimetric sensor based on peptide modified silver nanoparticles for determination of trypsin. Xu et al. [13] designed a fluorescence turn-on strategy

for trypsin detection based on FRET between AuNPs and C-dots. Shi et al. [12] reported a "turn-on" fluorescence system for determination of trypsin.

Compared with the single-signal method [14], dual-mode colorimetric and fluorescent nanoprobe [15–17] can offer two output modes and generate more accurate and reliable determination results. For instance, Shi et al. [15] proposed a dual-mode nanosensor for glutathione detection by using CQDs and AuNPs. Cheng et al. [16] reported a fluorescence and colorimetric dual-signal sensor based on gold nanoparticle for cyanide detection. Liu et al. [17] proposed a dual-signal sensor using inhibition of the growth of AuNP/CQDs composite for arginine detection.

AuNPs are widely applied in bioanalysis due to the distance-dependent color change and high efficiency of fluorescence quenching [9, 16]. Therefore, AuNPs are an excellent colorimetric indicator with color change from red to blue [18, 19]. AuNCs possess the characteristics of ultra-small size, good biocompatibility and high stability [20, 21]. Thus, AuNCs gained considerable attention as a novel fluorescent indicator. At present, there is no report on determination of trypsin using fluorescent and colorimetric dual-signal assay based on AuNCs and AuNPs. In this work, AuNCs and AuNPs were used to design a dual-signal approach for convenient, sensitive and selective determination of trypsin.

The detection strategy of dual-signal assay is illustrated in Scheme 1. After adding AuNCs into the AuNP solution, AuNPs were agglomerated. When Hb was added into the AuNPs solution, Hb coated the surface of AuNPs [22], thus protect AuNPs from being agglomeration. Because of the FRET between AuNCs and Hb-coated AuNPs, the fluorescence emission of Hb-coated AuNPs is quenched after the addition of AuNCs. AuNCs functioned as the fluorescent indicator and mediated AuNPs agglomeration, whereas AuNPs is used as the colorimetric indicator and fluorescent quencher. In the presence of trypsin, trypsin hydrolyzed Hb to polypeptides, which destroyed the coating of AuNPs by Hb. Therefore, AuNCs induced AuNPs agglomeration again, leading to the recovery of AuNCs fluorescence. Based on the change of fluorescence and absorbance, the concentration of trypsin can be determined. Thus, a nanoprobe system with high sensitivity and selectivity for detection of trypsin is established. This method delivers sensitive determination of trypsin in complicated biological environments such as human serum.

Materials and methods

Chemicals

Histidine ($C_6H_9N_3O_2$, ≥99.0%), auric chloride acid ($HAuCl_4$·$3H_2O$, ≥99.0%), trypsin, lysozyme, glucose oxidase, albumin from bovine serum, urase, ascorbic acid oxidase and acetylcholinesterase were purchased from Mackin (Shanghai, China, http://www.macklin.cn/). Hb (bovine blood) was obtained from Shanghai Biological Technology Development Co., Ltd. (Shanghai, China, http://shruji.company.lookchem.cn/). Sodium citrate ($C_6H_5Na_3O_7$·$2H_2O$, ≥99.0%) and hydrochloric acid were supplied by Chengdu Kelong Chemistry Reagent Factory (Chengdu, China, http://www.cdkelongchem.com/cn/). Trihydroxymethylaminomethane ($C_4H_{11}NO_3$, 99.5%-101%) was supplied by Wuxi Toptry Bio-Technology Co., Ltd. (Wuxi, China, http://www.ebiochemicals.com/). Ultrapure (UP) water used throughout the syntheses and analyses obtained with a Millipore system (18.23 MΩ·cm, Ulupure, China). All chemicals were used without further purification.

Apparatus and characterization

High resolution transmission electron microscopy (HRTEM) and transmission electron microscopy (TEM) were used to characterize the AuNCs and AuNPs with JEOL-2100F field emission transmission electron microscope (Japan), respectively. Fluorescence spectra of AuNCs were collected with a Perkin-Elmer LS55 spectrophotometer (USA) with 365 nm excitation and emission in the range of 385–650 nm. UV-Vis absorption spectra of AuNPs were measured on an AnalytikJena Specord200Plus spectrophotometer (Germany) from 400 nm to 750 nm. XPS was performed with ESCALAB 250XI multifunctional photoelectron spectrometer (USA). Zeta potential and dynamic light scattering (DLS) data were acquired on a Malvern Zetasizer instrument (UK) at room temperature.

Synthesis of AuNCs and AuNPs

AuNCs and AuNPs were synthesized according to previous report with minor modifications [23, 24]. Detailed synthesis steps are available in the Electronic Supporting Material.

Detection of trypsin

Trypsin standard solution with various concentrations were added into Tris-HCl buffer (10 mM, pH 8.0). Solutions consisting of 50 μL trypsin standard solution with different concentrations (0 ng·mL^{-1}-3500 ng·mL^{-1}) and 100 μL Hb at the optimal concentration (140 nM) were incubated for 20 min at 37 °C. Then 1 mL AuNP solution was added into the mixture solution, which was diluted to 2 mL with Tris-HCl buffer (10 mM, pH 7.0). Finally, 1 mL AuNC solution was added into the mixture solution. The mixture was kept at room temperature for another 45 min. The fluorescence spectra and UV-Vis absorbance were then collected.
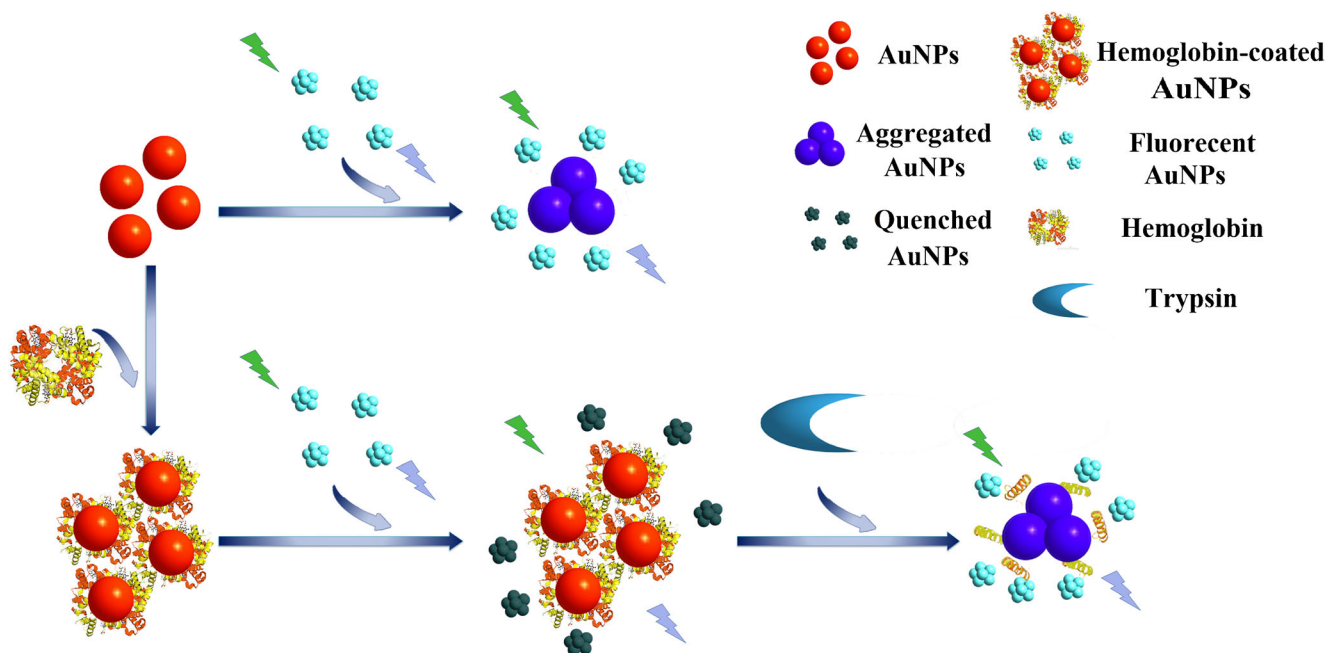
Scheme 1 Schematic diagram of the AuNC/AuNPs based fluorometric and colorimetric dual-signal assay for detection of trypsin

Serum samples analysis

To evaluate the practicability, human serum samples were collected to detect trypsin using the current method. The serum samples were collected from Chengdu First People's Hospital. All serum samples were obtained by legal means. The 500 μL serum sample contains Hb (140 nM) and Tris-HCl buffer (10 mM, pH 8.0). The mixture solution was incubated at 37 °C for 20 min. Then 1 mL AuNP solutios was added and Tris-HCl buffer (10 mM, pH 7.0) was used to dilute the solution to 2 mL. 1 mL AuNC solution was added to the solution. Finally, the UV-Vis absorbance spectra and fluorescence were collected after the mixture solution was kept at room temperature for 45 min. For the recovery test, 50 μL (200 ng·mL^{-1}, 500 ng·mL^{-1}, 1000 ng·mL^{-1}, 2000 ng·mL^{-1}) trypsin was mixed with spiked sample and the same procedures were followed.

Results and discussion

### Characterization of the AuNCs and AuNPs

In the HRTEM images (Fig. 1a), the spherical morphology of AuNCs with an average size of 2 nm is shown. According to the TEM images of AuNPs, both citric acid modified AuNPs (Fig. 1b) and Hb-coated AuNPs (Fig. 1c) have good dispersion with an average diameter of approximately 13 nm. As shown in Fig. 1d, after the AuNCs were added into AuNP solution, AuNCs can induce the aggregation of AuNPs. However, when Hb was present in the solution, it binds to the AuNPs surface and protects AuNPs from being

agglomerated (Fig. 1e). In presence of trypsin, Hb was hydrolyzed and the encapsulation of AuNPs by Hb was destroyed by trypsin. After AuNCs were added to solution, AuNPs were agglomerated again (Fig. 1f).

The average sizes of these particles were characterized by DLS. The average diameters of AuNCs (Fig. S2a), AuNPs (Fig. S2b) and the Hb-coated AuNPs (Fig. S2c) were 2.33 nm, 18.17 nm and 24.36 nm, respectively. It should be noted that the DLS data represents the hydrodynamic diameter of the hydration state of the nanoparticles, while the TEM image shows the actual size of the nanoparticles. Therefore, compared to the diameter measured by TEM, the diameter measured by the DLS method was significantly larger [25]. XPS survey spectrum shows that AuNPs (Fig. S3a) have two distinct peaks at 83.7 eV and 87.5 eV, respectively. For AuNCs (Fig. S3b), there are two peaks at 84.2 eV and 87.9 eV, The binding energy of Au4f$_{7/2}$ revealed that Au (0) and Au (I) are both present in AuNPs and AuNCs [26].

The AuNCs have a zeta potential of +6.0 mV (Fig. S4), which indicated the positively charged AuNCs were formed, while the AuNPs have a zeta potential of - 18.5 mV. The Hb-coated AuNPs have a zeta potential of - 25.4 mV. It means that Hb-coated AuNPs were negatively charged and the stability of Hb-coated AuNPs were further improved compared to AuNPs. The positively charged AuNCs tend to have electrostatic interaction with negatively charged AuNPs. Thus, AuNCs induced AuNPs agglomeration. The electrostatic interaction between AuNCs and Hb-coated AuNPs can induce the FRET between AuNCs and Hb-coated AuNPs, resulting in the quenching of AuNCs fluorescence. As shown in Fig. 2a curve A, the emission ranges from 385 to 650 nm, the maximum emission is at 455 nm, and the

Fig. 1 **a** HRTEM image of
AuNCs, **b** TEM image of AuNPs,
c TEM image of Hb-coated
AuNPs, **d** TEM image of AuNPs
in presence of AuNCs, **e** TEM
image of AuNPs in presence of
Hb and AuNCs, **f** TEM image of
AuNPs in presence of Hb, trypsin
and AuNCs
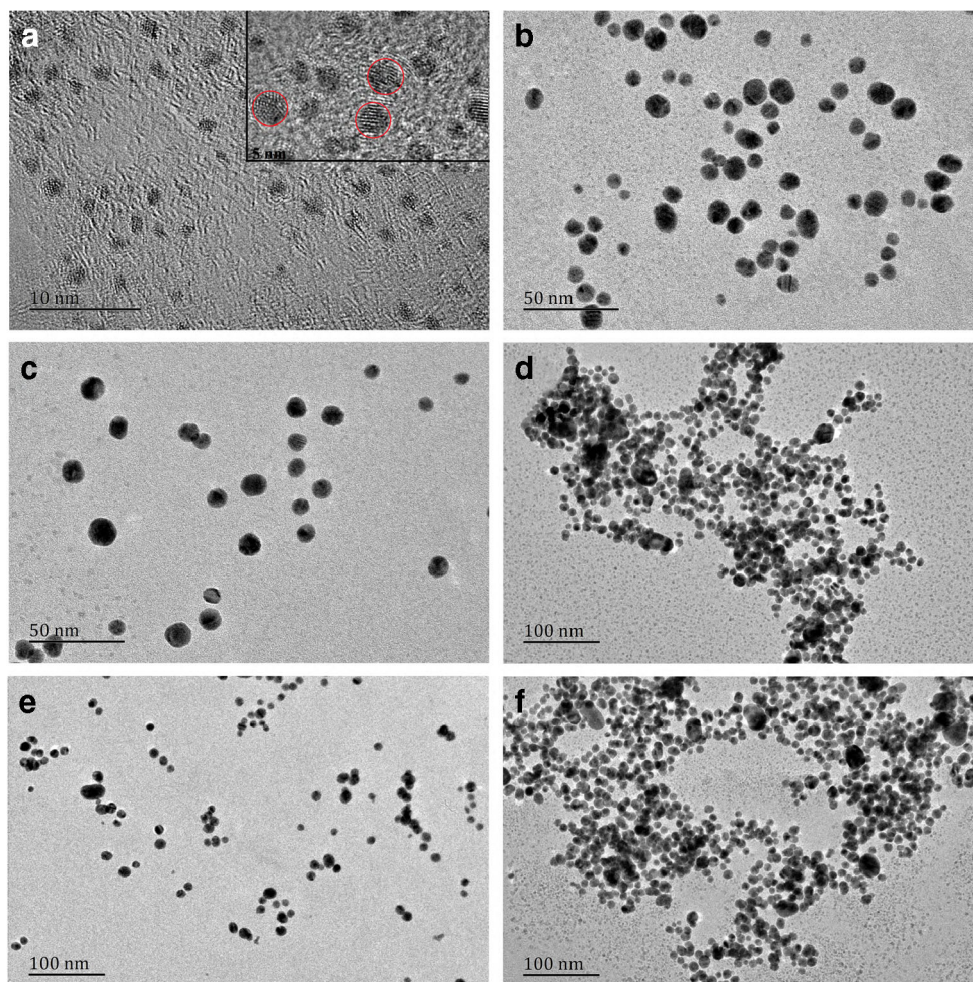
maximum excitation for the fluorescence of AuNCs is at 365 nm
(Fig. 2a curve B). In curve E of Fig. 2b, a broad absorption band
(300–800 nm) and the maximum absorption at 520 nm of the
AuNPs UV-Vis absorption spectrum is shown.

Detection mechanism and condition optimization

The mechanism of this dual-signal assay is illustrated in
Scheme 1. In this nanoprobe system, the surface of AuNCs
was modified by histidine, which contains imidazole and
amino group. The citric acid modified AuNPs have carbox-
yl group on the surface. Therefore, AuNCs and AuNPs
tend to have electrostatic interaction. Adding AuNCs into
AuNP solution can induce AuNPs to be agglomerated,
causing the AuNPs color transformation from red to blue
with the reduced distance between AuNPs. However, Hb
molecules can bind onto the AuNPs surface [22, 27], lead-
ing to the encapsulation of AuNPs. Therefore, the presence
of Hb can enlarge the distance between AuNPs and protect
AuNPs from being agglomerated after addition of AuNPs.
Because the fluorescence emission of AuNCs (455 nm
maximum emission) overlap with the Hb-coated AuNPs

UV-Vis absorption spectrum (Fig. S5) [13, 28], there was
fluorescence resonance energy transfer (FRET) between
Hb-coated AuNPs (as energy acceptors) and AuNCs (as
energy donors), which induced fluorescence quenching of
AuNCs. When trypsin was present in the solution contain-
ing Hb and AuNPs, Hb on AuNPs surface was hydrolyzed
into peptides [12], thus destroying the encapsulation of Hb
on AuNPs. After AuNCs were added to the solution,
AuNCs induced AuNPs aggregation again, thus the fluo-
rescence of AuNCs recovered because of decreased FRET
between AuNPs and AuNCs.

Fluorescence and UV-Vis absorption characterizations were
performed for testing the feasibility of this nanoprobe system.
The maximum fluorescence emission of AuNCs (Fig. 2a curve
B) is at 455 nm. When trypsin (Fig. 2a curve D) and Hb (Fig. 2a
curve C) were added to AuNCs, the fluorescence peaks of
AuNCs hardly changed, indicating that there was no molecular
interaction between Hb or trypsin and AuNCs. Figure 2b
depicted the absorption spectra in this nanoprobe system, and
the absorption spectra of AuNCs is shown as curve A in Fig. 2b.
The maximal UV-Vis absorption peak of AuNPs is at 520 nm
(Fig. 2b curve I). When AuNCs were added to Hb-coated
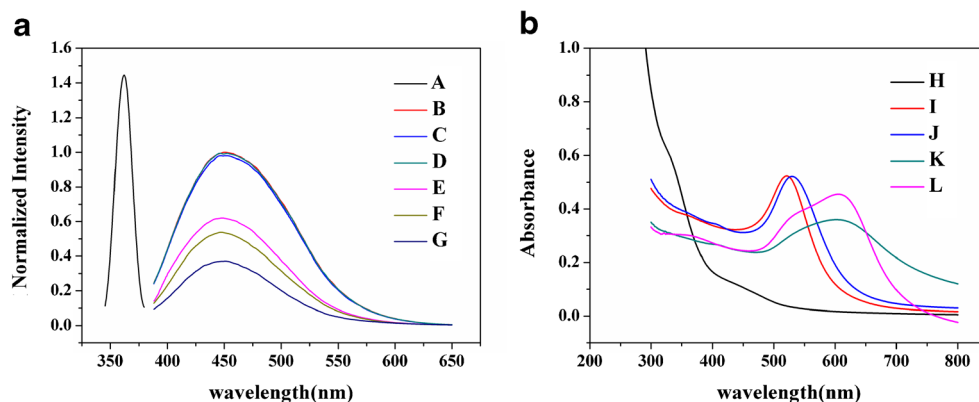
AuNPs, due to FRET between AuNCs and Hb-coated AuNPs, the AuNCs fluorescence was dramatically quenched (Fig. 2a curve G) and the maximal AuNPs UV-Vis absorption peak shifted slightly to 530 nm (Fig. 2b curve J). Trypsin can catalyze the decomposition of Hb on the surface of AuNPs, and AuNCs were added to induce AuNPs agglomeration, causing the maximum UV-Vis absorption peak from 530 nm to 610 nm with the AuNPs color changed from red to blue [29, 30] (Fig. 2b curve K). Therefore, the FRET effect between AuNPs with AuNCs was decreased, and the fluorescence effectively recovered (Fig. 2a curve E). In the control group, when AuNCs were added to AuNPs without Hb and trypsin, the maximum AuNPs UV-Vis absorption peak also red-shifted to 610 nm (Fig. 2b curve L), and the AuNCs fluorescence partially recovered compared with the circumstance when AuNCs were added to AuNPs with Hb (Fig. 2a curve F).

Fig. S1 shows after adding different concentrations of Hb into the system to coat AuNPs, the fluorescence (Fig. S1a) and UV-Vis absorbance (Fig. S1c) changed. There is a linear relationship between fluorescence (F/F_0-1) with the concentration of Hb (Fig. S1b), which means it is static quenching between Hb and AuNCs. With the increase of Hb concentration, the maximum absorption wavelength of AuNPs blue shifts to 530 nm in AuNCs. This means that Hb partially coats AuNPs, and the agglomeration induced by AuNCs is avoided. With the concentration of Hb at 140 nM, AuNPs were completely coated by Hb. Fig. S6 shows the UV-Vis absorbance and the fluorescence in this system with different reaction time. 45 min was selected as the optimal reaction time because the fluorescence and UV-Vis absorbance values maintained stable after 45 min. For obtaining the optimal pH value, the fluorescence and UV-Vis absorbance were measured in this system in the range of pH 5.0 and 10.0 (Fig. S7). Under the condition of pH 7.0, maximum response in fluorescence recover and UV-Vis absorbance were obtained.

Sensitivity and selectivity detection of trypsin

Under the optimal Hb concentration, reaction time and pH value, the nanoprobe system for trypsin detection by fluorescence emission and UV-Vis absorbance were investigated. Figure 3 shows that the maximum AuNCs fluorescence emission peak is at 455 nm, which increases with higher concentration of trypsin (0–3500 ng·mL-1) (Fig. 3a). Using (F/F_0-1) as the ordinate, the range from 10 ng·mL^{-1} to 2500 ng·mL^{-1} of the trypsin concentration as the abscissa (Fig. 3b), a linear relationship was established with a good correlation coefficient $(R^2 = 0.9939)$. Based on 3σ/S [31], the limit of trypsin detection (LOD) was 4.6 ng·mL^{-1}. The maximum UV absorption peak of AuNPs was 530 nm in this nanoprobe system with the optimal concentration of Hb (140 nM). As different concentrations of trypsin were added (0–3000 ng·mL^{-1}), the maximum UV absorption peak of AuNPs red-shifted and the intensity decreased, until reaching the maximum red-shift at 610 nm (Fig. 3c). The color of the mixture changed from red to blue. A linear correlation between the red-shift wavelength of AuNPs and the concentration of trypsin (20–2000 ng·mL^{-1}) was established (Fig. 3d). The detection limit based on 3σ/S is 8.4 ng·mL^{-1} and the linear correlation coefficient is $R^2 = 0.9926$. Compared with previously reported studies for trypsin detection, the present method exhibits significantly higher sensitivity and broader linear range (Table S1). Hence, this dual-signal assay provides more sensitive and reliable results than the traditional single-signal assay.

The selectivity of trypsin for fluorescence and UV-Vis absorption of this nanoprobe was also investigated. Potential interferents, including glycine (Gly), glutamic acid (Glu), phenylalanine (Phe), leucine (Leu), cysteine (Cys), glucose, ascorbic acid, dopamine, urea, glutathione, K^+, Na^+, Mg^{2+}, Cl^-, glucose oxidase (GOX), urease, ascorbic acid oxidase (AOX), acetylcholinesterase (AChE), lysozyme, albumin from bovine serum (BSA) (3000 ng·mL^{-1}) were added to the solution. Figure 4 shows that under equivalent experimental conditions, the fluorescence recover (Fig. 4a) and UV-Vis absorption (Fig. 4b) of trypsin (2000 ng·mL^{-1}) are much more significant than the interferents (3000 ng·mL^{-1}). Cysteine has an influence in the results of the system, but when cysteine and trypsin were mixed into the system, the fluorescence and colorimetric differed little from that with trypsin alone. Based on these results, it is verified that this method provides high selectivity for trypsin determination.

Fig. 3 a Fluorescence spectra of AuNPs, Hb (140 nM), AuNCs and different concentration of trypsin. **b** The plot of F/F_0–1 versus trypsin, the linear range for trypsin is 10–2500 ng·mL^{-1}, the inset photographs shows AuNPs in presence of Hb (140 nM), AuNCs and different concentration of trypsin under UV light (365 nm). **c** UV-Vis absorption spectra of mixture containing AuNPs, Hb (140 nM), AuNCs and different concentration of trypsin. **d** The plot of wavelength of maximum absorption versus trypsin concentration from 0 to 3000 ng·mL^{-1}, the linear response for trypsin is 20–2000 ng·mL^{-1}, the inset photograph shows the color of AuNPs in the presence of Hb (140 nM), AuNCs and different concentration of trypsin under natural light
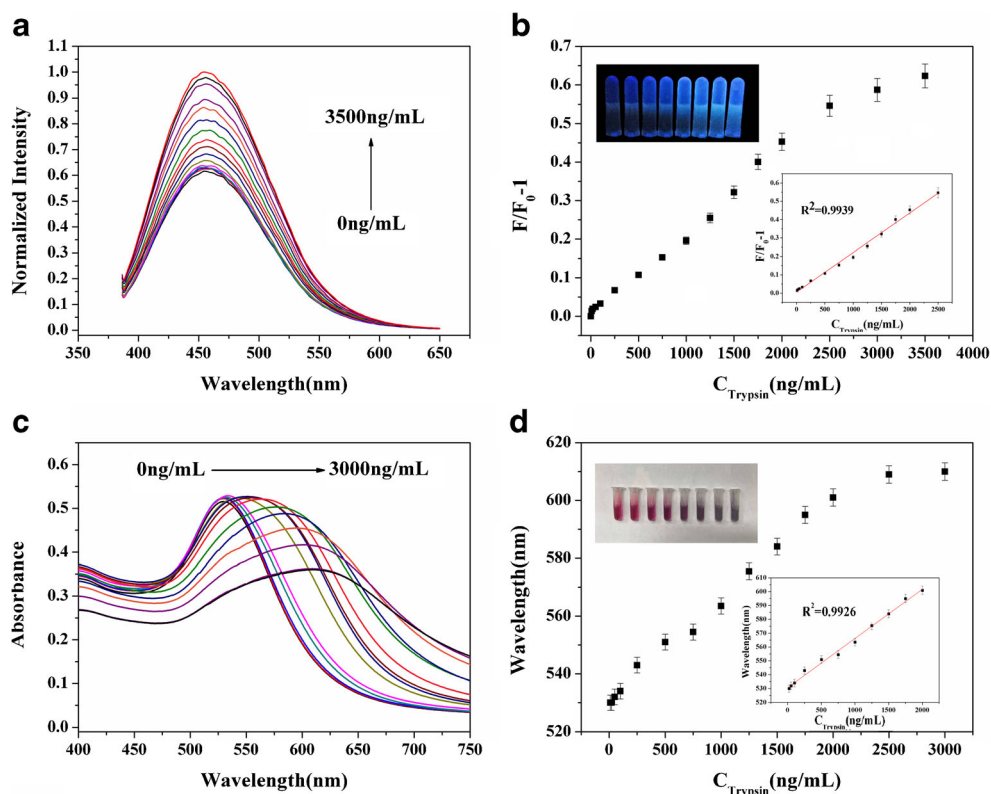
Detection of trypsin in human serum samples

For testing the practicability of the dual nanoprobe system of fluorescence emission and UV-Vis absorption for trypsin detection, trypsin in human serum collected from the First People's Hospital of Chengdu was determined using this nanoprobe system. All serum samples were obtained by legal means. In serum, the concentration of trypsin of healthy people is 248 ± 95 ng·mL^{-1} [32]. The fluorescence spectra of the Human Hemoglobin (HHb) exhibits the peak maxima at 322 nm ($\lambda_{ex} = 280$ nm) [33]. The maximum fluorescent emission of Human Serum Albumin (HSA) is at 343 nm ($\lambda_{ex} = 290$ nm) and the maximum peak of the UV absorption of HSA is at 278 nm [34], and both of them have little influence on the determination of trypsin in serum by fluorescence and colorimetry method. The test results of this nanoprobe system were compared with those by a commercial trypsin kit (Art. No. YX-C-B303) purchased from Sion Best Biological Technology Co., Ltd. As shown in Table 1, the results from this nanoprobe system is consistent with the results of the
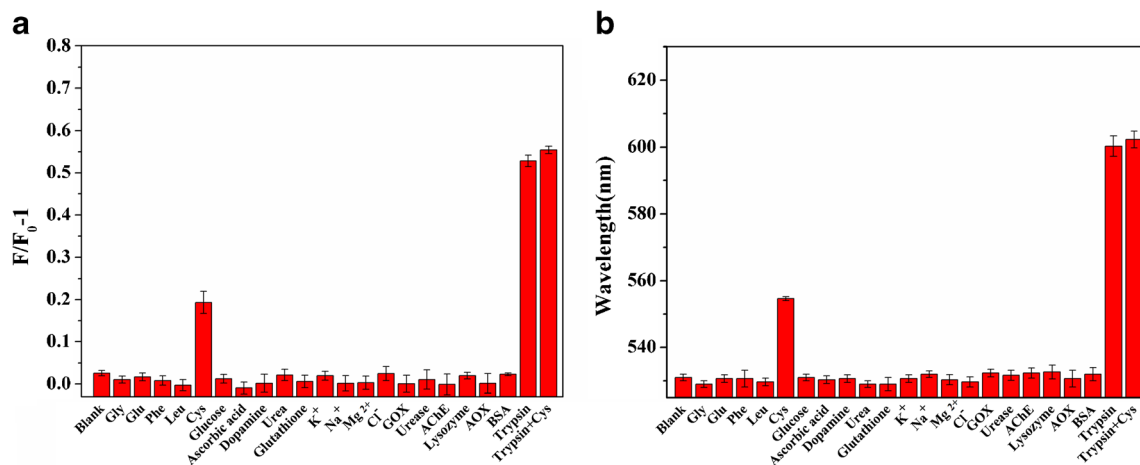

Fig. 4 a The fluorometric (F/F_0–1) response of nanoprobe in the presence trypsin (2000 ng·mL^{-1}) and various interferent species (3000 ng·mL^{-1}). **b** The wavelength of maximum absorption response of nanoprobe in the presence trypsin (2000 ng·mL^{-1}) and various interferent species (3000 ng·mL^{-1})

Table 1 The detection results of trypsin in human serum samples

Samples	Fluorometic				Colorimetric				Trypsin kit (ng·mL^{-1})
	Add (ng·mL^{-1})	Found (ng·mL^{-1})	Recovery (%)	RSD ($n = 3$, %)	Added (ng·mL^{-1})	Found (ng·mL^{-1})	Recovery (%)	RSD ($n = 3$, %)	
1	0	36.1	–	1.9	0	39.4	–	2.2	35.3
2	200	241.3	102.2	2.3	200	250.6	104.7	1.7	245.3
3	500	557.6	104.0	2.7	500	521.2	96.6	2.3	531.8
4	1000	1017.2	98.2	1.6	1000	1057.7	101.7	1.5	1034.6
5	2000	2013.7	98.9	2.0	2000	2030.8	99.6	2.1	2052.6

trypsin kit. Trypsin was diluted by 6 fold, and the measured concentration is 35.3 ng·mL^{-1} by trypsin kit, which means the real concentration of trypsin is 181 ng·mL^{-1} in human serum. For the fluorescence method, the recoveries range from 98.2%–104.0%, and RSDs range from 1.6%-2.7%. For the colorimetric method, the recoveries are in the range of 96.6%–104.7%, and RSDs are in the range of 1.5%–2.3%. Thus, this nanoprobe system offers sensitive and convenient determination of trypsin, and has high potential for practical application.

Conclusion

A new fluorescent and colorimetric dual-signal assay is developed for trypsin determination based on the gold nanocluster-induced aggregation of hemoglobin coated gold nanoparticles. By monitoring the maximum wavelength of AuNPs and fluorescence emitted by AuNCs, trypsin concentration can be determined. Broad linear ranges (10–2500 ng·mL^{-1} and 20–2000 ng·mL^{-1}) and low detection limitations (4.6 ng·mL^{-1} and 8.4 ng·mL^{-1}) were obtained for detection of trypsin. The present method demonstrates good sensitivity and selectivity for trypsin and has high potential for practical application in human serum.

Compliance with ethical standards The author(s) declare that they have no competing interests.

References

1. Deng Y, van der Veer F, Sforza S, Gruppen H, Wierenga PA (2018) Towards predicting protein hydrolysis by bovine trypsin. Process Biochem 65:81–92. https://doi.org/10.1016/j.procbio.2017.11.006

2. Zhu Q, Yu Z, Kabashima T, Yin S, Dragusha S, Elmahdy AFM, Ejupi V, Shibata T, Kai M (2015) Fluorometric assay for phenotypic differentiation of drug-resistant HIV mutants. Sci Rep 5:10323

3. Mao Y, Krischke M, Hengst C, Kulozik U (2018) Comparison of the influence of pH on the selectivity of free and immobilized trypsin for β-lactoglobulin hydrolysis. Food Chem 253:194–202. https://doi.org/10.1016/j.foodchem.2018.01.151

4. Te HS (2017) Metabolic and genetic liver diseases: Alpha-1 antitrypsin deficiency. In: Saeian K, Shaker R (eds) Liver disorders: a point of care clinical guide. Springer International Publishing, Cham, pp 329–338. https://doi.org/10.1007/978-3-319-30103-7_19

5. Temler RS, Felber J-P (1976) Radioimmunoassay of human plasma trypsin. BBA-Enzymol 445(3):720–728. https://doi.org/10.1016/0005-2744(76)90122-4

6. Lefkowitz RB, Marciniak JY, Hu C-M, Schmid-Schönbein GW, Heller MJ (2010) An electrophoretic method for the detection of chymotrypsin and trypsin activity directly in whole blood. Electrophoresis 31(2):403–410. https://doi.org/10.1002/elps.200900424

7. Šlechtová T, Gilar M, Kalíková K, Moore SM, Jorgenson JW, Tesařová E (2017) Performance comparison of three trypsin columns used in liquid chromatography. J Chromatogr A 1490:126–132. https://doi.org/10.1016/j.chroma.2017.02.024

8. Miao P, Liu T, Li X, Ning L, Yin J, Han K (2013) Highly sensitive, label-free colorimetric assay of trypsin using silver nanoparticles. Biosens Bioelectron 49:20–24. https://doi.org/10.1016/j.bios.2013.04.038

9. Xue W, Zhang G, Zhang D (2011) A sensitive colorimetric label-free assay for trypsin and inhibitor screening with gold nanoparticles. Analyst 136(15):3136–3141. https://doi.org/10.1039/c1an15224f

10. Chen H, Fang A, Zhang Y, Yao S (2017) Silver triangular nanoplates as an high efficiently FRET donor-acceptor of upconversion nanoparticles for ultrasensitive "turn on-off" protamine and trypsin sensor. Talanta 174:148–155. https://doi.org/10.1016/j.talanta.2017.06.006

11. Wu M, Wang X, Wang K, Guo Z (2017) An ultrasensitive fluorescent nanosensor for trypsin based on upconversion nanoparticles. Talanta 174:797–802. https://doi.org/10.1016/j.talanta.2017.07.013

12. Shi F, Wang L, Li Y, Zhang Y, Su X (2018) A simple "turn-on" detection platform for trypsin activity and inhibitor screening based on N-acetyl-l-cysteine capped CdTe quantum dots. Sensor Actuat B-Chem 255:2733–2741. https://doi.org/10.1016/j.snb.2017.09.087

13. Xu S, Zhang F, Xu L, Liu X, Ma P, Sun Y, Wang X, Song D (2018) A fluorescence resonance energy transfer biosensor based on carbon dots and gold nanoparticles for the detection of trypsin. Sensor Actuat B-Chem 273:1015–1021. https://doi.org/10.1016/j.snb.2018.07.023

14. Yang Y, Wang X, Liao G, Liu X, Chen Q, Li H, Lu L, Zhao P, Yu Z (2018) iRGD-decorated red shift emissive carbon nanodots for tumor targeting fluorescence imaging. J Colloid Interf Sci 509:515–521. https://doi.org/10.1016/j.jcis.2017.09.007

15. Shi Y, Pan Y, Zhang H, Zhang Z, Li M-J, Yi C, Yang M (2014) A dual-mode nanosensor based on carbon quantum dots and gold nanoparticles for discriminative detection of glutathione in human plasma. Biosens Bioelectron 56:39–45. https://doi.org/10.1016/j.bios.2013.12.038

16. Cheng C, Chen H-Y, Wu C-S, Meena JS, Simon T, Ko F-H (2016) A highly sensitive and selective cyanide detection using a gold nanoparticle-based dual fluorescence–colorimetric sensor with a wide concentration range. Sensor Actuat B-Chem 227:283–290. https://doi.org/10.1016/j.snb.2015.12.057

17. Liu T, Li N, Dong JX, Zhang Y, Fan YZ, Lin SM, Luo HQ, Li NB (2017) A colorimetric and fluorometric dual-signal sensor for arginine detection by inhibiting the growth of gold nanoparticles/carbon quantum dots composite. Biosens Bioelectron 87:772–778. https://doi.org/10.1016/j.bios.2016.08.098

18. Ma X, Gao L, Tang Y, Miao P (2017) Gold nanoparticles-based DNA logic gate for miRNA inputs analysis coupling Strand displacement reaction and hybridization chain reaction. Part Part Syst Charact:1700326

19. Ma X, Guo Z, Mao Z, Tang Y, Miao P (2018) Colorimetric theophylline aggregation assay using an RNA aptamer and non-crosslinking gold nanoparticles. Microchim Acta 185(1):33

20. Zhao D, Chen C, Zhao J, Sun J, Yang X (2017) Label-free fluorescence turn-on strategy for trypsin activity based on thiolate-protected gold nanoclusters with bovine serum albumin as the substrate. Sensor Actuat B-Chem 247:392–399. https://doi.org/10.1016/j.snb.2017.03.031

21. Hu L, Han S, Parveen S, Yuan Y, Zhang L, Xu G (2012) Highly sensitive fluorescent detection of trypsin based on BSA-stabilized gold nanoclusters. Biosens Bioelectron 32(1):297–299. https://doi.org/10.1016/j.bios.2011.12.007

22. Garabagiu S (2011) A spectroscopic study on the interaction between gold nanoparticles and hemoglobin. Mater Res Bull 46(12):2474–2477. https://doi.org/10.1016/j.materresbull.2011.08.032

23. Grabar KC, Freeman RG, Hommer MB, Natan M (1995) Preparation and characterization monolayers of au colloid monolayers, vol 67. https://doi.org/10.1021/ac00100a008

24. Yang X, Shi M, Zhou R, Chen X, Chen H (2011) Blending of HAuCl4 and histidine in aqueous solution: a simple approach to the Au10 cluster. Nanoscale 3(6):2596–2601. https://doi.org/10.1039/c1nr10287g

25. She W, Luo K, Zhang C, Wang G, Geng Y, Li L, He B, Gu Z (2013) The potential of self-assembled, pH-responsive nanoparticles of mPEGylated peptide dendron–doxorubicin conjugates for cancer therapy. Biomaterials 34(5):1613–1623. https://doi.org/10.1016/j.biomaterials.2012.11.007

26. Wu J, Jiang K, Wang X, Wang C, Zhang C (2017) On−off−on gold nanocluster-based near infrared fluorescent probe for recognition of cu(II) and vitamin C. Microchim Acta 184(5):1315–1324. https://doi.org/10.1007/s00604-017-2111-9

27. Shao Q, Wu P, Gu P, Xu X, Zhang H, Cai C (2011) Electrochemical and spectroscopic studies on the conformational structure of hemoglobin assembled on gold nanoparticles. J Phys Chem B 115(26):8627–8637. https://doi.org/10.1021/jp203344u

28. Bagdeli S, Rezayan AH, Taheri RA, Kamali M, Hosseini M (2017) FRET- based immunoassay using CdTe and AuNPs for the detection of OmpW antigen of Vibrio cholerae. J Lumin 192:932–939. https://doi.org/10.1016/j.jlumin.2017.08.032

29. Wang M, Wang L, Liu Q, Su X (2018) A fluorescence sensor for protein kinase activity detection based on gold nanoparticles/copper nanoclusters system. Sensor Actuat B-Chem 256:691–698. https://doi.org/10.1016/j.snb.2017.09.213

30. Chaudhary JP, Kumar A, Paul P, Meena R (2015) Carboxymethylagarose-AuNPs generated through green route for selective detection of Hg2+ in aqueous medium with a blue shift. Carbohyd Polym 117:537–542. https://doi.org/10.1016/j.carbpol.2014.10.016

31. Rao H, Ge H, Wang X, Zhang Z, Liu X, Yang Y, Liu Y, Liu W, Zou P, Wang Y (2017) Colorimetric and fluorometric detection of protamine by using a dual-mode probe consisting of carbon quantum dots and gold nanoparticles. Microchim Acta 184(8):1–9

32. J M A (1981) Serum trypsin levels in acute pancreatic and non-pancreatic abdominal conditions. Postgrad Med J 57(666)

33. Makarska-Bialokoz M (2018) Interactions of hemin with bovine serum albumin and human hemoglobin: a fluorescence quenching study. Spectrochim Acta A Mol Biomol Spectrosc 193:23–32. https://doi.org/10.1016/j.saa.2017.11.063

34. Ariga GG, Naik PN, Chimatadar SA, Nandibewoor ST (2017) Interactions between epinastine and human serum albumin: investigation by fluorescence, UV–vis, FT–IR, CD, lifetime measurement and molecular docking. J Mol Struct 1137:485–494. https://doi.org/10.1016/j.molstruc.2016.12.066

Affiliations

Zhengming Zhou[1] · Wei Liu[1] · Yanying Wang[1] · Fang Ding[2] · Xiaopeng Liu[3] · Qingbiao Zhao[4] · Ping Zou[1] · Xianxiang Wang[1] · Hanbing Rao[1]

1   College of Science, Sichuan Agricultural University, Xin Kang Road, Yucheng District, Ya'an 625014, People's Republic of China

2   Nanshan District Key Lab for Biopolymers and Safety Evaluation, Shenzhen Key Laboratory of Polymer Science and Technology, Guangdong Research Center for Interfacial Engineering of Functional Materials, College of Materials Science and Engineering, Shenzhen University, Shenzhen 518060, People's Republic of China

3   The Affiliated High School of Shanxi University, Wucheng West Road, Taiyuan 030006, People's Republic of China

4   Key Laboratory of Polar Materials and Devices, Ministry of Education, Department of Optoelectronics, East China Normal University, Shanghai 200241, People's Republic of China